

Constraints on star formation in the Taurus L1495 cloud from SPIRE/PACS observations of dense cores as part of the Herschel Gould Belt Survey



K. A. Marsh¹, J. M. Kirk², P. Palmeirim³, M. J. Griffin¹, D. Ward-Thompson²,
Ph. André³, A. Men'shchikov³, and HGBS team



1: Cardiff University, 2: University of Central Lancashire, 3: CEA-Saclay

Contact email: Ken.Marsh@astro.cf.ac.uk

Summary

- Catalogue of dense starless cores in L1495/B211/B213 region of Taurus Molecular Cloud, derived from *Herschel* PACS/SPIRE continuum images 70–500 μm (cf Palmeirim et al. 2013)
- SED fits to greybody dust models \Rightarrow mean dust temp., core mass, column density
- Classify core as gravitationally bound (prestellar) if mass $>$ (BE critical mass)/2 (Konyves et al. 2010)
- Largely complete for $M > 0.1 M_{\text{sun}}$ (prestellar) and $M > 0.02 M_{\text{sun}}$ (unbound cores, including those located in less dense, off-filament regions)
- All of the detected prestellar cores lie on filaments
- Prestellar core mass function (CMF) consistent with lognormal form
- Overall starless CMF (unbound + prestellar) is *not* lognormal
 - No evidence for low-mass turnover
- Density probability distribution function is lognormal except for high-density tail attributable to prestellar cores
 - Consistent with models of supersonic turbulence + self gravity

Herschel Gould Belt Survey

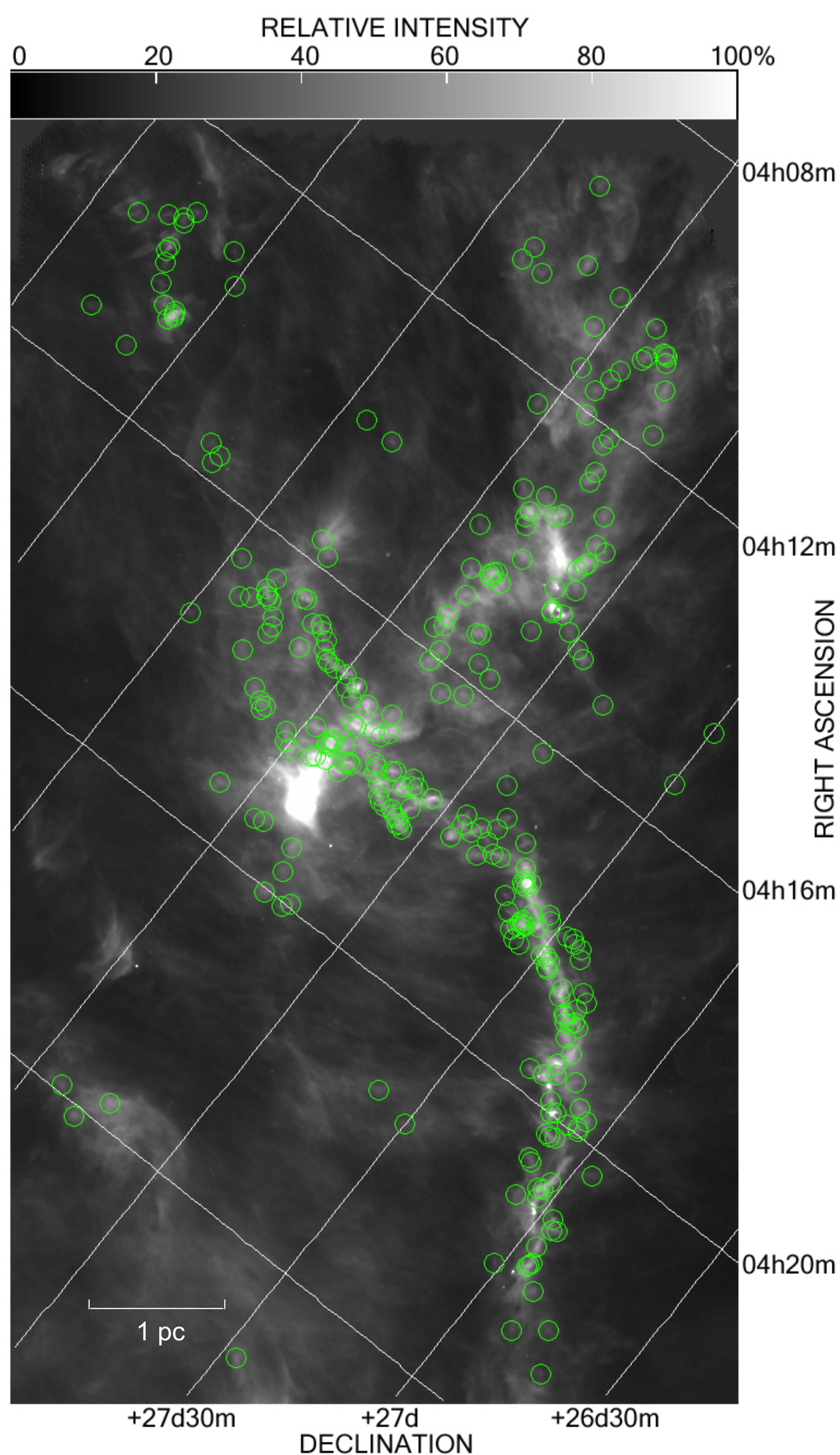
- Major goal: Characterize the prestellar CMF and the link between the CMF/IMF and cloud structure over the densest parts of Gould Belt (André et al. 2010)
 - 15 nearby molecular clouds, including Taurus
- Principal product: Catalogue of all detected dense cores & protostellar objects
 - Present work is one installment of the dense cores section of catalogue

Data analysis

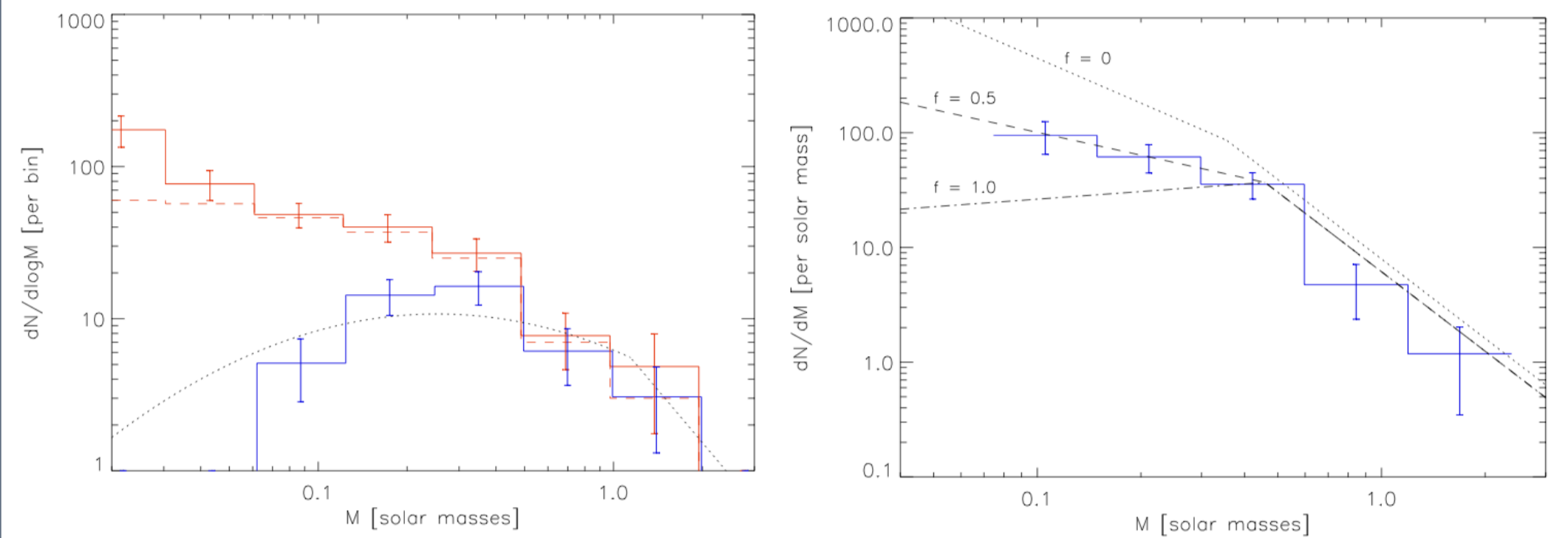
- Source detection via *getsources* (Men'shchikov et al. 2012)
- Source classification – principal conditions for classification as starless core:
 - robustly detected in 160–500 μm range & column density map *and*
 - not detected at 70 μm (to exclude protostellar objects) *and*
 - not coincident with known extragalactic object

Starless core locations on 250 μm continuum image

- Field of view = $4^\circ \times 2^\circ$
- Green circles represent all extracted sources classified as starless cores



Core Mass Function



Blue: Prestellar core CMF ($dN/d\log M$)

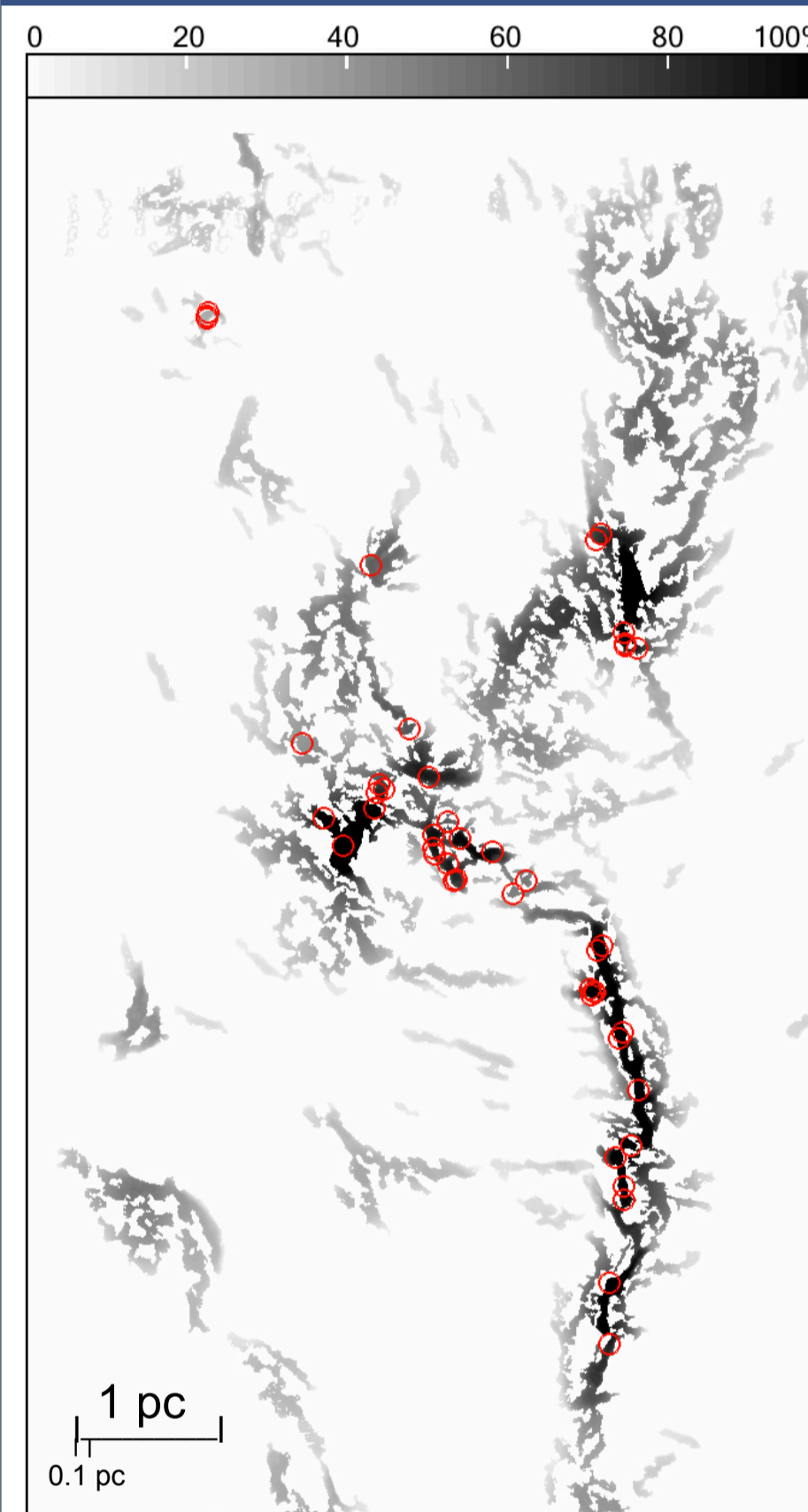
Red: Overall starless core CMF (solid: corrected for incompleteness; dashed: uncorrected)

Dotted: Chabrier (2003) stellar system IMF - scaled in mass by 1.15

Blue: Prestellar core CMF (in the alternate dN/dM representation to facilitate comparison with Kroupa's segmented power law IMFs)

Dotted, dashed, dash-dot: Kroupa (2012) stellar system IMFs (f = assumed binary frac.) - scaled in mass by 0.7

Prestellar core locations on filamentary column density map

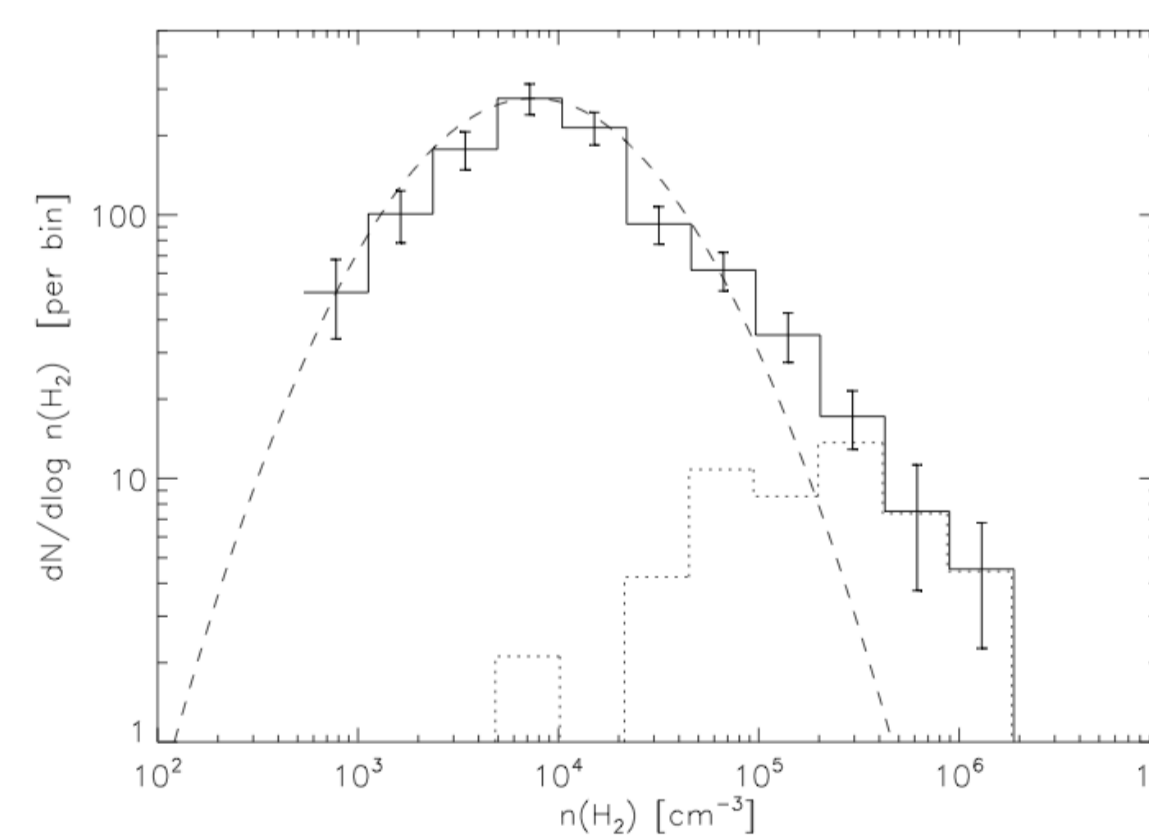


Greyscale represents column density of filamentary structures

- estimated using *getfilaments* (Men'shchikov 2013)
- 100% scale $\Rightarrow 15 M_{\text{sun}}/\text{pc}$
- Red circles represent prestellar core locations

Conclusion: All of the detected prestellar cores lie on filaments

Probability Distribution Functions



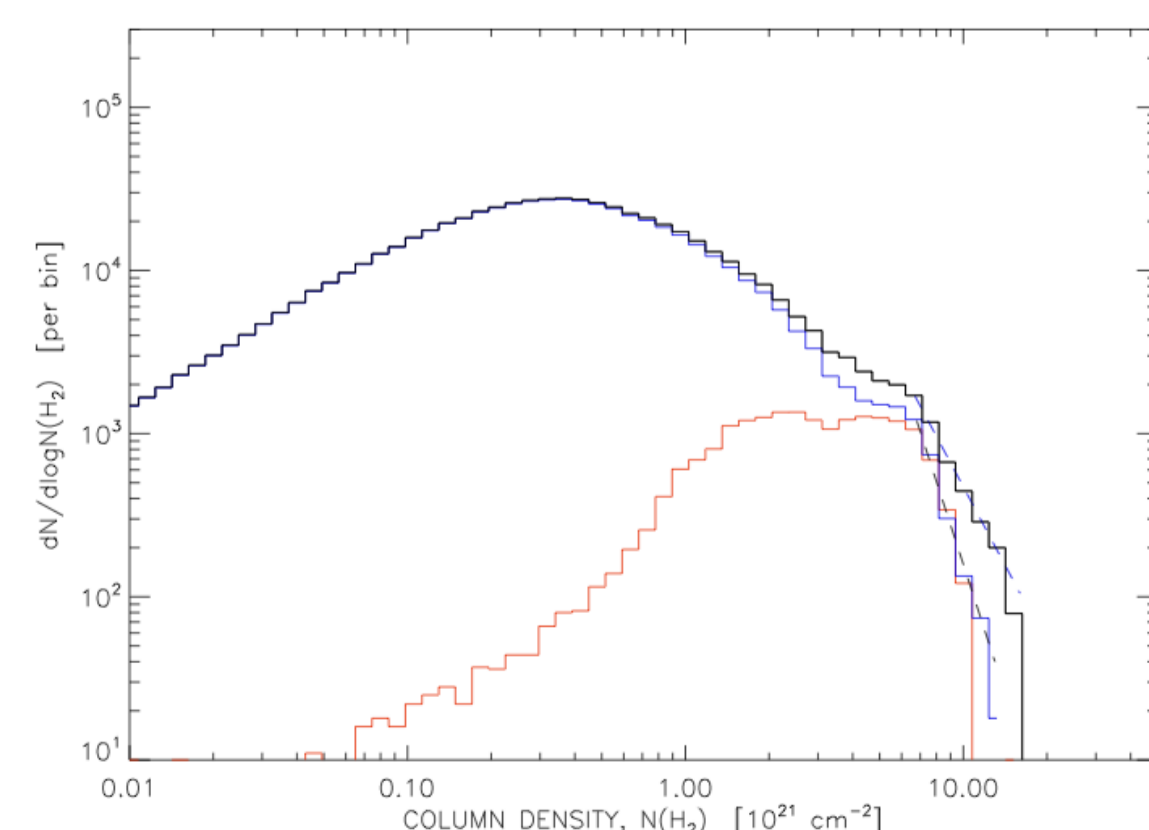
VOLUME DENSITY

Solid: All starless core extractions

Dotted: Prestellar cores only

Dashed: Lognormal, variance of log density, $s = 1.23$

Conclusion: Consistent with simulations of supersonic turbulence + gravity; power-law tail is due to prestellar cores (see e.g. Kritsuk et al. 2011)



COLUMN DENSITY (background-subtracted)

Black: All pixels

Red: Prestellar cores only

Blue: All pixels except for the immediate vicinity (within $60''$) of bright protostars

Conclusion: Prestellar cores account for only part of high column density tail; highest column densities are due to protostellar envelopes

References

- André, Ph. et al. 2010, *A&A*, 518, L102
Kritsuk, A. G. et al. 2011, *ApJ*, 727, L20
Men'shchikov, A. 2013, *A&A*, 560, A63
- Chabrier, G. 2003, *PASP*, 115, 763
Kroupa, P. et al. 2012, in *PS&SS*, 5
Palmeirim, P. et al. 2013, *A&A*, 550, A38
- Konyves, V. et al. 2010, *A&A*, 518, L106
Men'shchikov, A. et al. 2012 *A&A*, 542, 81